Nuclear Materials and Energy 21 (2019) 100702

Contents lists available at ScienceDirect

Nuclear Materials and Energy

journal homepage: www.elsevier.com/locate/nme

Plasma cleaning of steam ingressed ITER first mirrors

Kunal Soni*,[a], Lucas Moser[a], Roland Steiner[a], Daniel Mathys[b], Frederic Le Guern[c], Juan Piqueras[c], Laurent Marot[a], Ernst Meyer[a]

[a] Department of Physics, University of Basel, Klingelbergstrasse 82, CH-4056 Basel, Switzerland
[b] Swiss Nanoscience Institute, University of Basel, Klingelbergstrasse 50/70, CH-4056 Basel, Switzerland
[c] F4E, c/Josep Pla 2, Barcelona E-08019, Spain

ARTICLE INFO

Keywords:
ITER
First mirror
Steam ingress
Plasma cleaning
Reflectivity
XPS
Grain boundary

ABSTRACT

In ITER, the first mirrors (FMs) are vulnerable to an in-vessel coolant leak which could severely diminish their optical properties. To understand the scope of this potential impact, several FM samples were exposed to a steam and humidity test simulating the event in ITER. Both rhodium and molybdenum mirrors, observed a loss in specular reflectivity as a result (the loss being greater for the Mo mirror). Their surfaces were tarnished with the development a thin Rh oxide and a thick Mo oxide (120–170 nm). This study focusses on capacitively coupled radio frequency (CCRF) plasma cleaning of steam ingressed (SI) FM samples and follow their optical recovery. Plasma cleaning experiments were performed with 13.56 MHz CCRF plasma using argon and/or hydrogen as process gas (with 230 eV ion energy). Initial and final reflectivity measurements, chemical surface analysis using in vaccuo X-ray photoelectron spectroscopy, scanning electron microscopy, focused ion beam and roughness measurements, were carried out for each sample to evaluate the cleaning efficiency. Using the plasma cleaning technique, it was possible to remove the SI induced contamination from the mirror surfaces and recover their optical properties to the pristine levels. Several 'voids/inclusions' were seen to arise along the grain boundaries as a result of the SI procedure. The concentration of these 'voids/inclusions' was observed to increase till a certain point followed by a decrease with increasing cleaning time.

1. Introduction

Metallic First Mirrors (FMs) will play a critical role in the optical diagnostic systems of ITER. FMs will be the first elements in the optical path of the diagnostics that will allow the light from the fusion plasma to cross the neutron shielding. For this reason, FMs will be placed in close proximity to the fusion plasma exposing them to high particle fluxes and hence to surface erosion and/or deposition [1,2] which will substantially affect their optical properties. The net deposition of the particles sputtered from the first wall i.e. beryllium (Be) and tungsten (W) is a major concern, as it can severely degrade the optical properties of FMs and since FMs are the first elements in an optical labyrinth, the eventual reliability of the optical diagnostic will be compromised. To cope with such parasitic deposition, an in situ mirror cleaning technique will be implemented in ITER. Plasma and laser cleaning [3] are among the thoroughly researched techniques, with plasma cleaning being the most promising one [4].

For their capability of preserving good reflectivity under sputtering conditions, molybdenum (Mo) and rhodium (Rh) [5] either in mono- or nano-crystalline form are considered the prime candidates for ITER FMs [6]. One of the most effective ways of removing dust from the mirror surface by plasma sputtering is done using the mirror itself as the electrode, applying direct current (DC), pulsed DC or alternating current (AC) directly on it. The ionization of the process gas as a result, produces a local discharge. Research led by a group in Kurchatov Institute [7] used Penning discharge where DC or pulsed DC is applied on the FM which serves as cathode, the second mirror being the counter electrode. The system was able to efficiently clean 200 nm aluminium (Al) deposits from Mo mirror placed at discharge voltages upto 750 V. However DC caused surface charging of insulating deposits resulting in dielectric breakdown leading to severe degradation of the mirrors. This issue could be solved by employing pulsed DC. Another technique into achieving plasma cleaning is by feeding RF to the mirror (typically with frequencies between 13.56 and 81.4 MHz) in a capacitively coupled discharge, and is the subject of research of several laboratories around the world. Experiments have been performed in the past investigating the effectiveness of the technique both with and without magnetic fields with favorable outcomes. Research conducted at University of

* Corresponding author.
E-mail address: kunaldhirajal.soni@unibas.ch (K. Soni).

https://doi.org/10.1016/j.nme.2019.100702
Received 12 June 2019; Received in revised form 23 August 2019; Accepted 25 August 2019
Available online 29 August 2019

Basel in the past, led to successful cleaning of ITER relevant contaminants i.e. Al (as a Be proxy) and W from FM samples using argon (Ar) plasma [8]. Further, to test its efficacy on Be deposits, experiments were also conducted in the JET-BeHF with helium (He) and/or Ar plasma with positive results [9]. It was possible to significantly reduce the deposit thickness, often removing it completely and recovering the mirror reflectivity in turn. In a recent publication, the team reported successful cleaning of Be contaminated Rh and Mo mirrors using D_2 plasma at different ion energies [10]. The latest results from the group at Ioffe Institute in St. Petersburg showed promising results in using CCRF plasma cleaning without magnetic field [11]. They were able to establish a correlation between the applied frequency and the effective sputtering rates of contamination and mirror materials using the ion current density and ion energy distribution function. They also predicted He to be a good candidate for cleaning Mo mirrors from Be deposits, for its high Be/Mo sputtering rate ratio, in the frequency range of 80–100 MHz. A group from Institute of Plasma Physics in Hefei, China performed cleaning experiments on an edge Thompson scattering (ETS) mirror mock up in EAST tokamak to investigate the reliability of the CCRF plasma cleaning technique in tokamak environment with magnetic field [12]. Upon utilization of Ne plasma with a 1.7 T magnetic field in EAST tokamak, they were able to homogeneously remove aluminum oxide films (used as beryllium proxy). The reflectivity of the mirrors was fully recovered upon cleaning in EAST tokamak with magnetic field and the cleaning efficiency was found to be 40 times higher than without magnetic field. Finally, a group from TNO, Netherlands developed a mockup in representative geometry of the FM cleaning system for the Upper Wide Angle Viewing System (UWAVS) diagnostic in ITER [13]. With the application of 30–60 MHz RF discharges and He as the process gas, they were able to remove 10–20 nm thick Al coatings from FM samples at the rate of 1.5–3 nm/hour. Using similar parameters, they were also able to remove 10–20 nm thick W coatings from FM samples at a rate of 0.3–0.5 nm/hour [14]. These sputter rates were around 10 times lower than achieved with Ar as the process gas [8]. In their latest research they observed that upon plasma cleaning with the previous discharge parameters, the material sputtered from the FM was deposited at various locations and on the second mirror (SM) with an estimated rate of 0.05 nm/hour or lower [15]. Litnovsky et al. in a recently published article, gives a good overview of the recent developments in the work plan of the first mirror R&D [4].

Besides erosion and deposition, the FMs are also vulnerable to a 'Vacuum Vessel Ingress of Coolant Event' or VVICE in ITER [16]. The VVICE could occur from an accidental rupture of the cooling loops inside the vacuum vessel or damage of the cooling pipes due to runaway electrons generated during plasma disruptions. Following a VVICE, the FMs are expected to be exposed to steam from the leaked coolant, at pressures up to 1.5 bar and temperatures up to 250 °C (maximum temperature being during the ITER baking process). In addition, the steam will also mobilise dust, which could eventually get deposited on the mirror surfaces, further degrading the optical properties. Hence, in order to investigate the net impact of a VVICE event, several FM samples were subjected to a steam and humidity test simulating the event [17,18]. The process is also called steam ingress (SI) and the resulting samples, steam ingressed. Konovalov et al. conducted a study recently, where they analysed the effects of boiling water and steam on several metallic mirror samples [19]. They observed that the material of the mirror played a decisive role in the degree of impact of water and steam on mirror degradation and the resulting corroded layer could be successfully removed by bombardment with Ar ions of moderate energy and ion fluence.

This study is focussed on the plasma cleaning of Rh and Mo mirror samples, subjected to the steam and humidity test on the lines of VVICE conditions in ITER. It is worth noting that in ITER, the VVICE would most likely occur on mirrors which would already be contaminated with Be and W deposits from fusion plasma. However, after SI, the contaminated layer will mostly comprise of BeO and the plasma cleaning of BeO film has been demonstrated previously [20].

2. Experimental

2.1. Steam ingress

Three highly polished circular mirror samples of lab compatible sizes (diameter ϕ = 18–25 mm and thickness t = 4 mm), were used for the steam and humidity test. Two of them were nano-crystalline Rh mirrors (NcRh A and B, provided by two different companies) on a stainless steel (SS) substrate and the third sample, a single crystal Mo mirror (ScMo). To determine the Rh film thickness, a FIB measurement was performed on NcRh A and B, and was found as 800 and 350 nm, respectively. Although the Rh coating thickness was supposed to be identical, two different companies using magnetron sputtering technique [21] produced different films. Moreover their deposition parameters could be different, leading to different coating structures. For additional analysis, another set of same mirrors were also subjected to the steam and humidity test, referred to as SI#2 further in this paper. Also all instances of SI refer to SI#1 in this paper, unless stated otherwise. All the mirrors displayed a high total and a low diffuse reflectivity in their pristine states, similar to the one calculated using Palik optical constant [22]. The steam and humidity test involved subjecting the mirror samples to varying steam pressures and temperatures in a series of steps mimicking the expected conditions in ITER immediately after a water vessel leak. The test procedure, employed at Karlsruhe Institute of Technology, pursued the following steps: i. sample exposure to steam at pressure of 1.5 bar and temperature of 250 °C for 3 h, ii. decrease in temperature to 100 °C and pressure to 1 bar with exposure for 3 h, iii. increase in temperature to 200 °C, pressure being at 1 bar with exposure for 1 day, iv. decrease in temperature to 30 °C and exposure in 100% humidity with pressure at 1 bar for 1 week and, v. baking at 240 °C with 1 bar pressure for a minimum of 5 h until the atmosphere is dry.

2.2. Plasma cleaning

The cleaning procedure was performed in a high vacuum (HV) chamber at University of Basel (see Fig. 1 of reference [23]). The mirror was used as an electrode and the discharge was driven using CCRF. It consists of having the RF power applied on the mirror which allows it to achieve a desired self bias leading to ion sputtering. In the proceeding experiments, 13.56 MHz excitation frequency was feeded to the electrode. The negative self-bias on the mirror accelerates the positively charged ions towards it, causing them to sputter the surface. The sputtering yield can be increased or decreased by changing the discharge gas, as well as the plasma generating parameters. Moreover the plasma is positively charged (in a range of 25–40 V) which adds up with the self-bias to provide the ion energy (in eV). A power of 32 W led to a self bias of −200 V and an ion energy of 230 eV. The discharge conditions used in the experiments for the different mirrors can be found in Table 1.

Table 1
Discharge conditions used for the plasma cleaning experiments.

Mirror sample	Discharge gas	Partial pressure (Pa)	Cleaning time (hour)
NcRh A	Ar	0.5	12.5
NcRh B	Ar	0.5	16
	H_2	1	14
ScMo	H_2 + Ar (1:1)	1 (0.5 + 0.5)	16
	Ar	0.5	4

2.3. Characterization techniques

The surface chemical composition of the samples was characterized using X-ray photoelectron spectroscopy (XPS). The samples were transferred *in vacuo* from the experimental chamber to an ultra high vacuum chamber for XPS analysis [23]. The electron spectrometer is equipped with a hemispherical analyzer (Leybold EA10/100 MCD) and a non-monochromatized Mg Kα X-ray source (hν = 1253.6 eV) was used for core level spectroscopy. The binding energy (B.E.) scale was calibrated using the Au 4f7/2 line of a cleaned gold sample at 84.0 eV. The fitting procedure of core level line is described in Ref. [24]. A profilometer (TENCOR alpha-stepper 500) was used to measure the surface roughness. The ex situ UV-Vis-NIR total and diffuse reflectivity (250–2500 nm) of the mirrors was recorded using a Varian Cary 5 spectrophotometer. The specular reflectivity could be calculated by subtracting the diffuse component from the total reflectivity. The morphology of mirrors post cleaning processes was investigated using a scanning electron microscope (SEM, Hitachi S-4800 field emission at 5 kV) and focused ion beam (FIB, Helios NanoLab 650).

3. Results and discussion

3.1. Post steam ingress characterization

Following the steam ingress, the mirrors were characterized thoroughly. The characterization techniques included XPS, ex situ reflectivity, roughness, SEM and FIB analysis.

3.1.1. Single crystal molybdenum mirror

The effect of SI was quite drastic on the ScMo mirror. Visually, the mirror exhibited strong surface deterioration. Upon further analysis with the spectrophotometer, it was established that post SI, the total reflectivity decreased from 74% for pristine mirror to 15% at λ = 250 nm, while the diffuse reflectivity increased slightly (Fig. 1a) in the visible region at λ = 500 nm. All the reflectivity values discussed further in this paper shall correspond to λ = 250 nm unless stated otherwise. The net specular reflectivity decreased from 73% to 12% (Fig. 1d). The increase in diffuse reflectivity often corresponds to an increase in surface roughness (Bennet's law [25]). In our case, the roughness R_q was measured as 64 nm, indicating a fairly rough surface morphology. To analyze the chemical composition of the surface, an XPS measurement was performed, which revealed the presence of carbon (C), nitrogen (N) and oxygen (O) (at B.E. 284.7 eV, 398.6 eV and 530.5 eV respectively) on the sample surface in addition to Mo. The presence of C, N and O on the surface is expected since the sample was exposed to air prior to its XPS measurement. As can be observed in Fig. 2a, the Mo3d core level spectra obtained, was deconvulated in one doublet corresponding to MoO_3 [24]. The B.E. and atomic concentrations of Mo and its oxide/s can be found in Table 2. The formation of MoO_3 on surface upon high temperature steam oxidation of Mo is in accordance with literature [26]. The large drop in total reflectivity is a result of the formation of the oxide layer. The oxide layer was further analysed using FIB, where the thickness of the oxide layer (distinguishable grainy layer in Fig. 3) was found to be in the range of 120–170 nm. The diffusion length of oxygen in Mo, taking into account the time and temperature of the SI precedure steps, was also calculated theoretically using Fick's law of diffusion [27,28] for comparison and was found to be 291 nm. The theoretical diffusion length is higher than the measured 120–170 nm, since the diffusion equation [27] takes into account a pure oxygen environment unlike the steam and humidity test. However, the order of the two diffusion lengths (theoretically calculated and the one measured after steam and humidity test) are the same.

3.1.2. Nanocrystalline rhodium mirror

In case of NcRh A and B, the visual change was not very apparent. However, the specular reflectivity decreased from 69% for pristine mirror to 35% (Fig. 1d), with both the total reflectivity decreasing from 70% to 44% and the diffuse reflectivity increasing from 1% to 9% (Fig. 1b and c). Similar reflectivity drop was also obtained in thick Rh coated mirror samples (Rh coating between 4–5μm, not shown here) upon SI. Since such thick mirrors will compose the FM units in ITER diagnostic systems, it calls for a detailed investigation in the SI and subsequent cleaning process. The presence of C, N and O was revealed on the surface by XPS analysis (at B.E. 284.4 eV, 398.9 eV and 531.5 eV respectively) in addition to Rh (consequence of air exposure). The core level Rh3d spectrum obtained was deconvoluted in two components, whose B.E. corresponded to Rh metal and oxide [29]. The B.E. and atomic concentrations of Rh and its oxide can be found in Table 3. The low atomic concentrations of Rh oxide signaled to a very thin layer of surface oxide. The thickness of the oxide could not be measured using the FIB cross section images, however since it was detected by XPS in low concentrations, we believe it to be lower than the XPS analysis depth (< 3 nm). To further study the surface properties, the sample topography was analysed using SEM. The SEM images of both NcRh A and B revealed a surface covered with contaminant particles as analysed with XPS (Fig. 4b). However, examining the cross section of the Rh coating using FIB revealed the presence of several 'voids/inclusions' along the depth of the mirror (Fig. 4e). While 'voids' will be used for reference further in the article, the idea of inclusions should be considered as well. These voids were also observed in thick Rh coated mirrors after SI (Fig. 4f). It was also seen that while for the thin Rh coated mirrors, the voids occurred throughout the thickness of the mirror, for the thick Rh coated (ITER relevant) mirrors, the voids mainly occurred in the top 500 nm along the depth. Since no such voids were observed along the cross section of the pristine mirror (Fig. 4d), it can be concluded they arose as a result of the SI process. While the voids were not visible on the surface immediately after SI, a light Ar plasma cleaning of the surface unveiled their presence on the surface too. They were formed in deeper regions (after a depth of approximately 10 nm) in the mirror and the initial Ar plasma cleaning allowed the etching of that top layer to unveil the voids on the surface. The voids mainly occurred along the grain boundaries of both the NcRh mirrors. The high physical stress experienced by the outer surface in the steam environment combined with the thermal stress experienced by the sample during the SI procedure could be responsible for the observations. These voids could be associated with the phenomenon of grain boundary migration or dislocations which also arise under extreme physical and thermal stress, and have been studied before [30]. The formation of voids on the surface could also explain the increase in the diffuse reflectivity of the samples. An increase in diffuse reflectivity should follow an increase in surface roughness according to Bennet's law. However, R_q was found to be 7 nm, which pointed to a fairly smooth surface topography. This contradiction arises due to the fact that the diameter of the stylus tip of the profilometer (= 2 μm) which measures the roughness by scanning over the sample surface, was roughly 100 times larger than the size of the 'voids' which were in the range of 10–100 nm. Due to a larger tip diameter, the profilometer doesn't take into consideration the contribution of voids while measuring the surface roughness. It is worth noting that these voids arose only in coated mirrors and not single crystalline mirror as characterized earlier, pointing to the idea that this phenomenon is only associated with nanocrystalline mirrors. This fact was confirmed by exposing a Mo coated mirror in SI test, which also developed voids along the thickness of the coating. The generation of voids is an important observation with regard to optical diagnostics in ITER, as it points to physical damage at the grain level of thin film mirrors in the event of SI and is worth further analysis.

3.2. Plasma cleaning: ScMo mirror

The plasma cleaning of the ScMo mirror sample was performed in several stages using hydrogen (H_2) and Ar gases to study their

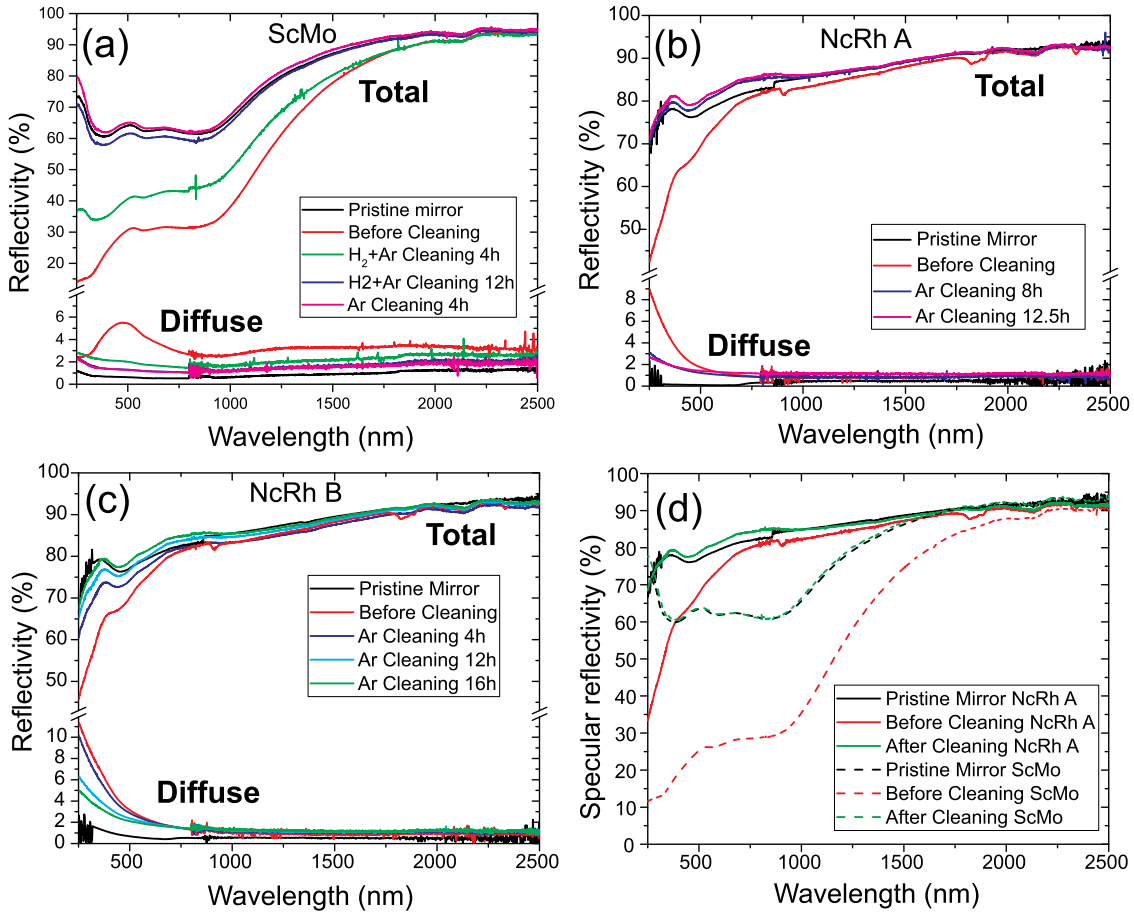

Fig. 1. Total and diffuse reflectivity of (a) single crystal molybdenum mirror, (b) nanocrystalline rhodium mirror A, (c) nanocrystalline rhodium mirror B during different phases of plasma cleaning and (d) specular reflectivity of ScMo and NcRh A (NcRh B being similar) in pristine state, before and after plasma cleaning.

sputtering impact on Mo. To begin with, the cleaning was done in a pure H_2 plasma to study its sputtering effect on Mo. In a further stage Ar was added to the H_2 plasma in an equal ratio (1:1) in terms of partial pressure, to increase the physical sputtering yield on Mo and the process was concluded with cleaning in pure Ar.

H_2 plasma is able to reduce the oxidation state of surface MoO_3 via chemical sputtering of O atoms. To study its impact, ScMo was cleaned in H_2 plasma with parameters described in Table 1. The XPS measurement after the first cleaning exhibited a complete removal of the C and N. Mo3d peaks were shifted to lower values indicating a reduction of the oxidation state. The spectrum was deconvulated into three components. The BE of the components corresponded to three different oxidation states of Mo as seen in Fig. 2b, namely MoO_3, MoO_2 and MoO_x, the latter corresponding to a reduced oxide [31]. With 230 eV H^+ ions, the sputtering yield of Mo is of the order 10^{-5} atoms/ion [32] and a similar order is expected for MoO_3 as well, which is insufficient for the complete removal of the oxide film.

Chemical sputtering, by nature, involves chemical reactions between target and projectile atoms which leads to formation of new species that are loosely bound to the surface and more easily sputtered. This form of sputtering at best can reduce the oxidation state of the surface species. For a more efficient cleaning, it is necessary to deploy physical sputtering, which involves momentum transfer from the impinging projectiles to target atoms. Hence, to increase the physical sputtering yield, Ar was added to H_2 plasma in a 1:1 partial pressure ratio. Ar is able to etch the Mo surface by physical sputtering and has a sputtering yield of 0.27 atoms/ion which is 10^4 times larger than H_2. After the second cleaning, a lower amount of O (Table 2) was measured by XPS as well as a shift of Mo3d to a lower B.E., corresponding to Mo in metallic state and a reduced oxide (Fig. 2c). Moreover, the specular reflectivity recovered significantly after the second cleaning. As can be observed in Fig. 1a, the total reflectivity increased from 15% before cleaning to 70% after cleaning while the diffuse reflectivity attained the pristine mirror levels.

To conclude the cleaning process with a higher sputtering yield, the sample was cleaned in a pure Ar plasma. The cleaning was finished with pure Ar and not H_2, as the latter was found to negatively impact the reflectivity of virgin Mo or Rh mirrors by forming hydrides [24]. After the final cleaning step, XPS measurement reported a further decrease in the O concentration along with a single Mo3d doublet whose peak BE referred to metallic Mo as shown in Fig. 2d. The specular reflectivity also recovered completely as seen in Fig. 1d. The roughness R_q at the end of the cleaning process also reduced significantly to 20.2 nm, in contrast to 64 nm before cleaning, establishing a smoother surface. The visual transformation of the mirror upon plasma cleaning can be seen in Fig. 5a and b.

3.3. Plasma cleaning: NcRh mirror A and B

NcRh samples A and B were cleaned in pure Ar plasma using identical cleaning parameters (Table 1). However the time for complete optical recovery required by the two mirrors were different.

The Rh3d spectrum of NcRh A, obtained by XPS, upon deconvolution led to a single doublet whose peak BE matched that of pure Rh metal confirming the removal of the oxide layer. The specular reflectivity of the sample recovered to 90% of the pristine mirror values after 8 h of cleaning. The sample was further cleaned for 4.5 h for a complete recovery. The total and diffuse reflectivity of the mirror after

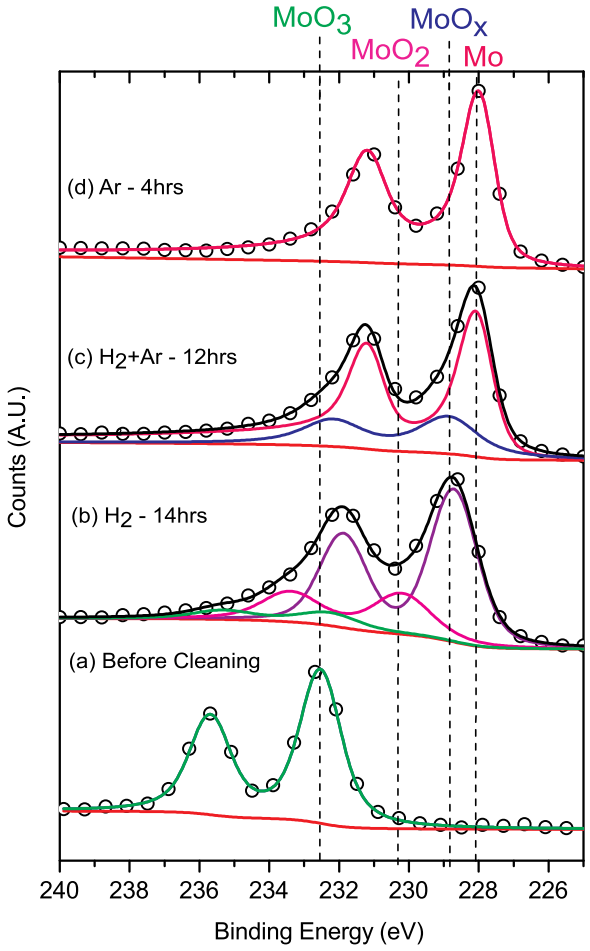

Fig. 2. Mo3d core level spectra of the ScMo mirror sample (a) before cleaning, (b) after a 14 h plasma cleaning with hydrogen gas, (c) after an additional 12 h plasma cleaning with a 1:1 mixture of hydrogen and argon gas and (d) after an additional 4 h plasma cleaning with only argon gas. The dashed vertical lines represent the binding energies of the different oxidation states of Mo. The coloured lines represent the different components. The open circles are the spectrum data points after background subtraction, where one of every ten data points are presented. The solid line behind the open circles is the fit sum of the components.

Table 2
Binding energies and atomic concentrations of chemical species on ScMo mirror as measured by XPS for the cleaning steps.

		Mo	MoO_3	MoO_2	MoO_x	O
B.E. (eV)		228.1	232.6	230.2	228.8	530.5
		Atomic concentration (%)				
Cleaning process	Before cleaning	0	26.5	0	0	73.5
	H_2–14 h	0	4.1	12.4	33.8	43
	H_2 +Ar–12 h	54	0	0	18	27
	Ar–4 h	89	0	0	0	11

the cleaning had completely recovered reaching the pristine mirror levels as can be seen in Fig. 1b. Similar observations were recorded for NcRh B as well. Although, the XPS measurements done after 4 h of cleaning affirmed the removal of oxide layer, the specular reflectivity of the sample was completely recovered only after 16 h of cleaning (Fig. 1d). The visual transformation of the mirror upon plasma cleaning can be seen in Fig. 5c and d.

To track the etching rate of the Rh coating, FIB measurements were

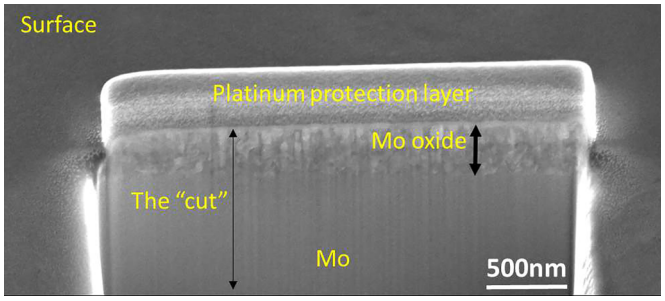

Fig. 3. FIB cross section of ScMo showing the oxide layer on the Mo surface. A Pt layer was deposited prior to making the FIB cut to protect the mirror surface.

Table 3
Binding energies and atomic concentrations of chemical species on NcRh A and B as measured by XPS for the cleaning steps.

	NcRh A			NcRh B		
	Rh	Rh oxide	O	Rh	Rh oxide	O
B.E. (eV)	307.2	307.6	531.4	307.1	307.9	531.5
	Atomic concentration (%)					
Before cleaning	47.4	14.4	38.2	59.2	5.6	35.2
After cleaning	100	0	0	100	0	0

done along the cleaning steps. It was found that the Rh coating for both NcRh A and B, was etched off at the rate of 15 nm/hour upon Ar plasma sputtering. An ion flux corresponding to this plasma had been measured in this facility previously and was found to be 2.9×10^{19} atoms.m^{-2}.s^{-1} [8]. At this etching rate 187.5 nm and 240 nm of mirror material from NcRh A and B was removed respectively. Although this represents a large portion of the initial thickness of the test mirrors, the mirrors to be used in ITER would be in the order of 10 μm. A thickness of that order is sufficient to sustain the 15 VVICE projected to occur in ITER lifetime.

The topography of the samples was analysed using SEM after each cleaning cycle to track the evolution of 'voids' which were observed in the post SI characterization. Since the SEM characterization of the samples subjected to SI#1 was only started after at least 4 hours of Ar plasma cleaning, a second set of same samples was subjected to SI#2 to analyse the void phenomenon immediately after SI. Upon subsequent cleaning steps, the concentration of 'voids' on the surface was first seen to increase in both NcRh mirrors till a certain point followed by a phase of decrease with further cleaning (Fig. 6). The profile indicated that the highest concentration of voids existed several nanometers below the surface. The void concentration profile along the depth was, however, different for the two mirrors. Upon prolonged plasma cleaning the void concentration decreased and it was possible to recover a surface free of voids. However in doing so, a large portion of the mirror was etched away. Moreover, as the void concentration decreased later with increasing cleaning time, the diffuse reflectivity was seen to decrease, pointing to a correlation between the two. Generation of voids upon SI could result in an increase in the diffuse reflectivity due to enhanced light scattering. Hence upon extended cleaning, as the void concentration decreased, the diffuse reflectivity decreased as well (as observed in Fig. 1b and c).

4. Conclusion and outlook

Following a steam and humidity test of Rh and Mo first mirror samples, a thin Rh oxide and a thick Mo trioxide (120–170 nm) layers emerged on their surfaces. This led to a drop in the specular reflectivity of both Rh and Mo mirrors, the latter being affected much more than the former. Using 13.56 MHz CCRF plasma cleaning at 230 eV with Ar

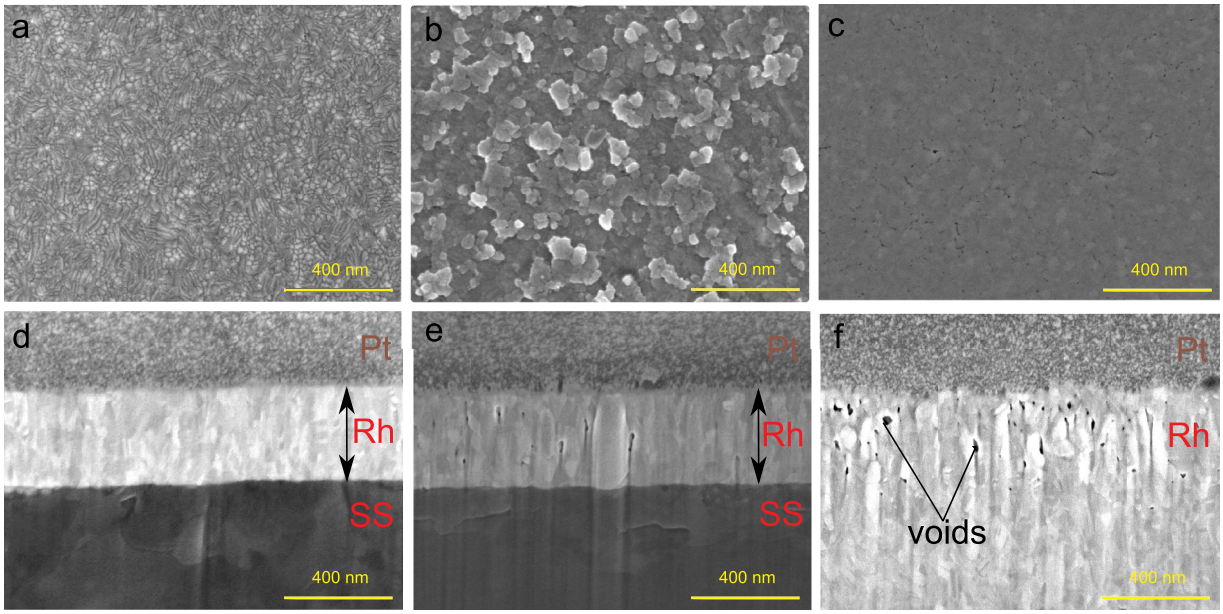

Fig. 4. SEM images along the timeline of NcRh B: (a) surface of the pristine mirror sample, (b) surface of the mirror after SI depicting the contamination, (c) surface of the mirror at the end of 16 h Ar plasma cleaning depicting a reduced concentration of voids, (d) cross section of the pristine mirror sample showing the Rh coating, (e) cross section of the sample after SI displaying the voids along the thickness of the coated Rh (Similar images and trend were also observed for NcRh A) and (f) cross section of a thick Rh coated mirror (4.1 μm) relevant for ITER operations, displaying voids after SI ; Pt: platinum protection layer applied during FIB, Rh: rhodium coating and SS: stainless steel substrate.

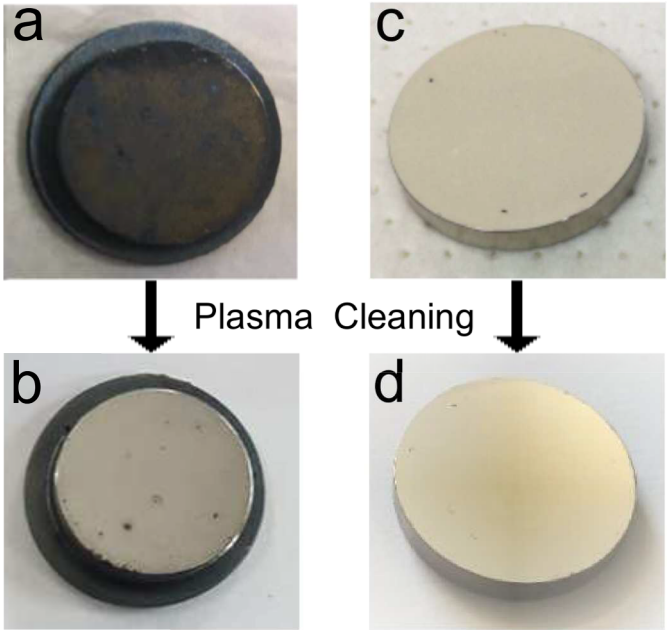

Fig. 5. ScMo (a) before cleaning and (b) after 30 h of H_2 and/or Ar plasma cleaning. NcRh A (c) before cleaning and (d) after 12.5 h of Ar plasma cleaning. NcRh B also appeared similar to NcRh A before and after plasma cleaning.

and/or H_2 as the process gas, it was possible to recover the specular reflectivities of both Rh and Mo mirrors to their pristine states. Rh coated mirrors were etched at a rate of 15 nm/hour with Ar plasma sputtering. Moreover, the Rh mirrors, being nanocrystalline, had developed 'voids/inclusions' in the range of 10–100 nm along their grain boundaries due to the thermal and physical stress experienced during the steam and humidity test. These voids existed along the thickness of the nanocrystalline mirrors. Upon plasma cleaning, the concentration of the voids first increased to a certain point followed by a decrease with further increase in the duration of the plasma cleaning. The diffuse

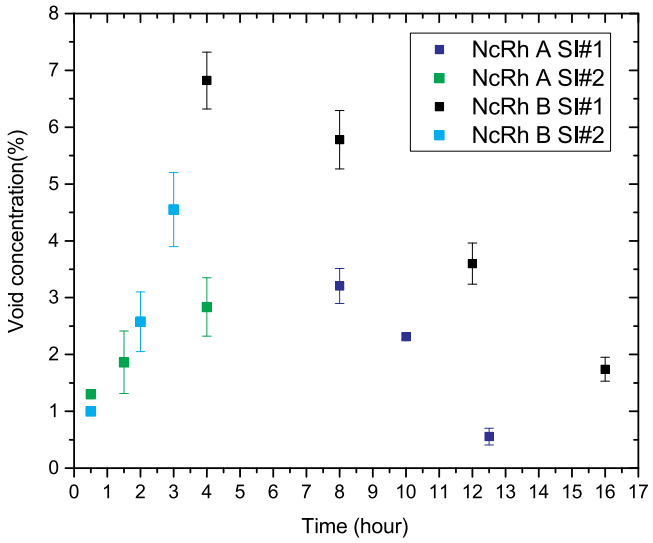

Fig. 6. Variation of the hole density of the sample surface with the duration of plasma cleaning. SI#1 and SI#2 refer to the samples subjected to two independent SI tests with same test parameters conducted at different times.

reflectivity of the mirrors is most likely linked to the presence of voids. The phenomena of void formation was not observed in single crystalline mirrors. SI test was also performed on a Mo coated mirror sample (not shown in the paper) which also developed voids. This leads us to believe that the nano crystalline structure of the mirror (both Rh and Mo) is prone to void formation. While the presence of voids seemed to negatively influence the optical properties of FMs, it was possible to completely recover the specular reflectivity of the NcRh mirrors with plasma cleaning. Additional experiments are required for a detailed study of void origination along the grain boundaries upon exposure to steam induced stress. Furthermore, plasma cleaning, depending on driving frequency and ion energy, typically has an inhomogeneity degree that can range from 20–40% (the centre being sputtered more than the sides). While this does not affect the mirror over a single sputtering

cycle, it could lead to a modification in the original geometry of its surface upon multiple cleaning cycles as projected over the lifetime of ITER and needs to be considered for the design of FMs.

5. Data availability

The raw/processed data required to reproduce these findings cannot be shared at this time as the data also forms part of an ongoing study.

Declaration of competing interest

The authors declare that they have no known competing financial interests or personal relationships that could have appeared to influence the work reported in this paper.

Acknowledgments

The authors would like to thank A.Pereira and P.Martin from CIEMAT, Spain, and R.Lopez from INTA, Spain for conducting the characterization of the samples before and after the steam and humidity test and providing the data for our research. Swiss Federal Office of Energy, Swiss Nanoscience Institute, Swiss National Science Foundation and the Federal Office for Education and Science are acknowledged for their financial support. This publication reflects the views only of the author, and Fusion for Energy cannot be held responsible for any use which may be made of the information contained therein.

Supplementary material

Supplementary material associated with this article can be found, in the online version, at doi:10.1016/j.nme.2019.100702.

References

[1] E.E. Mukhin, et al., First mirrors in ITER: material choice and deposition prevention/cleaning techniques, Nucl. Fusion 52.1 (2011) 013017.
[2] M. Walsh, et al IEEE/NPSS 24th Symposium on Fusion Engineering, 2011, Chicago, IL, 26–30 June (2011) http://ieeexplore.ieee.org/xpl/articleDetails.jsp?arnumber=6052210.
[3] A. Maffini, et al., In situ cleaning of diagnostic first mirrors: an experimental comparison between plasma and laser cleaning in ITER-relevant conditions, Nucl. Fusion 57.4 (2017) 046014.
[4] A. Litnovsky, et al., Diagnostic mirrors for ITER: research in the frame of international tokamak physics activity, Nucl. Fusion 59.6 (2019) 066029.
[5] A. Litnovsky, et al., Diagnostic mirrors for ITER: A material choice and the impact of erosion and deposition on their performance, J. Nucl. Mater. 363 (2007) 1395–1402.
[6] L. Marot, et al., Optical coatings as mirrors for optical diagnostics, J. Coat. Sci. Technol. 2.3 (2016) 72–78.
[7] A.V. Rogov, Y.V. Kapustin, A.G. Alekseev., Application of the penning discharge for cleaning mirrors in optical diagnostics of the ITER, Instrum. Exp. Tech. 58.1 (2015) 161–166.
[8] L. Moser, et al., Towards plasma cleaning of ITER first mirrors, Nucl. Fusion 55 (2015).
[9] L. Moser, Plasma cleaning of beryllium coated mirrors, Phys. Scr. T167 (2016) 14069.
[10] M.B. Yaala, et al., Deuterium as a cleaning gas for ITER first mirrors: experimental study on beryllium deposits from laboratory and JET-ILW, Nucl. Fusion 59.9 (2019) 096027.
[11] A.M. Dmitriev, et al., In situ plasma cleaning of ITER diagnostic mirrors in noble-gas RF discharge, Phys. Scripta 2017 (T170) (2017) 014072.
[12] R. Yan, L. Moser, B. Wang, J. Peng, C. Vorpahl, F. Leipold, R. Reichle, R. Ding, J. Chen, L. Mu, R. Steiner, E. Meyer, M. Zhao, J. Wu, L. Marot, Nucl. Fusion 58 (2018) 026008.
[13] A. Ushakov, et al., UWAVS first mirror plasma cleaning technology using 30–60 MHz RF discharges, Fusion Eng. Des. 131 (2018) 54–60.
[14] A. Uskhakov, et al., Removing W-contaminants in helium and neon RF plasma to maintain the optical performance of the ITER UWAVS first mirror, Fusion Eng. Des. 136 (2018) 431–437.
[15] A. Ushakov, A. Verlaan, R. Ebeling et al., UWAVS first mirror after long plasma cleaning: Surface properties and material re-deposition issues, *Fusion Eng. Des.*, In press, corrected proof, Available online 6 March 2019.
[16] R.L. Frano, et al., Experimental investigation of functional performance of a vacuum vessel pressure suppression system of ITER, Fusion Eng. Des. 122 (2017) 42–46.
[17] A. Pereira, et al., SG07 d04 steam and humidity test report, idm@f4e UID / VERSION 28KEAR / 1.0, VERSION CREATED ON 16 may, 2017,. EXTERNAL REFERENCE P0000034819.
[18] J.A. Gonzalo, et al., 33rd ITPA diagnostics, ITER, France, 2017, https://portal.iter.org/departments/POP/ITPA/Diag/DIAG/Document%20Library/36/Presentations/08-06-AlonzoGozalo.pdf.
[19] Konovalov, et al., Effects of water impact on optical properties of metallic mirror samples, Probl. Atomic Sci. Technol. 25 (2019) 41–44. No 1. Series: Plasma Physics.
[20] L. Moser, et al., Investigation and plasma cleaning of first mirrors coated with relevant ITER contaminants: beryllium and tungsten, Nucl. Fusion 57.8 (2017) 086019.
[21] M. Joanny, et al., Achievements on engineering and manufacturing of ITER first-mirror mock-ups, IEEE Trans. Plasma Sci. 40.3 (2012) 692–696.
[22] E.D. Palik, G. Ghosh, Handbook of Optical Constants of Solids, Academic, New York, 1985.
[23] M. Wisse, et al., Spectroscopic reflectometry of mirror surfaces during plasma exposure, Rev. Sci. Instrum. 83.1 (2012) 013509.
[24] B. Eren, et al., The effect of low temperature deuterium plasma on molybdenum reflectivity, Nucl. Fusion 51 (2011).
[25] H.E. Bennett, J.O. Porteus, Relation between surface roughness and specular reflectance at normal incidence, JOSA 51.2 (1961) 123–129.
[26] E.S. Jones, et al., The oxidation of molybdenum*, Corrosion 14 (1) (1958) 20–26.
[27] V.I. Baranova, S.A. Golovin, M.A. Krishtal, M.I. Lerner, Inelastic phenomena in molybdenum due to diffusion, Country unknown/Code not available: N. p. (1968). Web.
[28] P. Heitjans, J. Kärger, Diffusion in condensed matter: Methods, Materials, Models, Springer, 2005, pp. 5–6.
[29] Y. Abe, et al., Rhodium and rhodium oxide thin films characterized by XPS, Surf. Sci. Spectra 8.2 (2001) 117–125.
[30] R.C. Gifkins, Grain boundary migration in high-temperature deformation, Cryst. Res. Technol. 19.6 (1984) 809–818.
[31] A.D. Gandubert, et al., X-ray photoelectron spectroscopy surface quantification of sulfided comop catalysts-relation between activity and promoted sites-part i: influence of the co/mo ratio, Oil Gas Sci. Technol.-Revue de l'IFP 62.1 (2007) 79–89.
[32] B. Rainer, W. Eckstein (Eds.), Sputtering by particle bombardment: experiments and computer calculations from threshold to MeV energies, Vol. 110 Springer Science and Business Media, 2007, p. 72.